GEOPHYSICAL RESEARCH LETTERS, VOL. 23, NO. 5, PAGES 519-522, MARCH 1, 1996

An estimate of the surface shortwave cloud forcing over the western pacific during TOGA COARE

Duane E. Waliser

Institute for Terrestrial and Planetary Atmospheres, State University of New York, Stony Brook

William D. Collins

Center for Clouds, Chemistry and Climate, Scripps Institution of Oceanography, La Jolla, California

Steven P. Anderson

Department of Physical Oceanography, Woods Hole Oceanographic Institution, Woods Hole, Massachusetts

Abstract. Estimates of the shortwave cloud forcing at the surface have been computed for the TOGA COARE Intensive Observation Period (IOP) using the IMET buoy surface insolation measurements. Two different methods have been employed to calculate the clear-sky surface insolation. The first is based on an empirical approximation using the buoy observations. The second incorporates both modeling and empirical procedures. The net surface shortwave cloud forcing values derived from these two methods are -103 and -107 Wm^{-2}, respectively. These values indicate that for the COARE IOP, the surface cooling effect from shortwave cloud forcing is comparable to that from latent heat flux (-108.5 Wm^{-2}). Comparing IOP values of OLR and MSU rain rate to their climatological values indicates that the mean cloudiness during the IOP corresponds closely to climatology, suggesting that these estimates of shortwave cloud forcing may be fairly representative of the climatological value.

Introduction

One of the primary objectives for the Tropical Ocean Global Atmosphere (TOGA) Coupled Ocean Atmosphere Response Experiment (COARE; Webster and Lukas, 1992) was to quantify cloud-surface feedbacks in the western Pacific. In this study, we use TOGA COARE data to estimate the impact of clouds on the surface energy budget of the western Pacific warm pool. Specifically, we compute the effects of clouds on the downwelling, upwelling and net shortwave radiation at the surface, and discuss how the net shortwave cloud forcing estimates compare with other components of the surface heat budget during TOGA COARE, and how closely they might represent the climatological cloud forcing value.

Data

The primary data set used in this study is the downwelling shortwave observations from the IMET buoy moored at 1.75°S and 156°E during the TOGA COARE IOP (R. Weller, personal communication, 1995). The observations were measured by an Eppley radiometer located at a height of 3.5m above the mean water line on the buoy. The time series used in this study consists of 7.5 minute averages and extends from October 22, 1992 to March 3, 1993 with a four-day gap in early December.

Additional supporting data includes the International Satellite Cloud Climatology Project (ISCCP) DX data collocated with the IMET buoy. This data set is used to filter out cloudy periods from the buoy time series in order to determine and/or validate the estimates of the clear-sky surface flux. The DX version of ISCCP was specifically processed for the TOGA COARE period and consists of a pixel-level retrieval analysis at the resolution of the ISCCP B3 product (Rossow and Schiffer, 1991). For this study, only data from the Japanese GMS geostationary satellite are used. The 3-hour DX data has a resolution of 30 km, although the data within any one grid cell comes from a single satellite pixel with a resolution of approximately 5 km. The specific data used for this application includes the cloud-detection flag and the visible reflectance from the grid cell located at 1.7°S and 156.1°E.

Precipitable water estimates derived from the Special Sensor Microwave/Imager (SSM/I; Schluessel and Emery, 1990) are used to determine the uncertainty in our estimate of shortwave cloud forcing introduced by the variability in atmospheric water vapor. These data include all samples within 0.5° of the buoy location from both the F-10 and F-11 DMSP satellites.

Two long-record proxies of cloudiness are used to determine whether the TOGA COARE period tended to be more or less cloudy than climatology. The first consists of a twenty-one year, monthly time series of Outgoing Longwave Radiation (OLR; Gruber and Krueger, 1984). The OLR data have a 2.5° spatial resolution, and the grid cell used here is from 2.5°S and 156.25°E. The second proxy consists of a fifteen year record of oceanic precipitation derived from the Microwave Sounding Unit aboard the NOAA meteorological satellites (Spencer, 1993). These data also have a 2.5° spatial resolution and the time series used here is from 1.25°S and 155°E.

Methods

The effect of clouds on the shortwave radiation budget at the surface can be expressed by:

$$C_{sd} = SW_a\downarrow - SW_c\downarrow \quad (1)$$

$$C_{su} = \alpha_a SW_a\downarrow - \alpha_c SW_c\downarrow \quad (2)$$

C_{sd} and C_{su} represent the effect of clouds on the downwelling and upwelling shortwave radiation at the surface, respectively.

Paper number 96GL00245
0094-8534/96/96GL-00245$03.00

$SW_a\downarrow$ and $SW_c\downarrow$ represent the all-sky and clear-sky downwelling shortwave radiation at the surface. α_a and α_c represent the all-sky and clear-sky surface albedos. The net effect of the clouds on the surface energy budget is determined by the difference between C_{sd} and C_{su}, i.e., $C_{sn} = C_{sd} - C_{su}$.

We use two methods to determine $SW_c\downarrow$. The first scheme filters out cloudy periods from the buoy time series and then computes an empirical relationship between clear-sky flux and the cosine of the solar zenith angle [hereafter, $\cos(\theta_o)$] from the remaining "clear-sky" samples. The cloud screening is based on the ISCCP DX data in accordance with the following criteria. First, the time of the buoy sample must fall within the 3-hour time span of an ISCCP sample where the cloud flag for the previous, current and subsequent ISCCP samples are all equal to zero. Second, additional constraints are imposed on the visible reflectance. After the above filter is applied, the reflectance values for the remaining samples range up to 0.045 for $\cos(\theta_o) < 0.7$, and up to 0.115 for $\cos(\theta_o) >= 0.7$. The second criterion filters out samples with a visible reflectance greater than 0.022[1] for $\cos(\theta_o) < 0.7$ and greater than 0.038[1] for $\cos(\theta_o) >= 0.7$. Since the ocean is generally much less reflective than clouds, this criterion simply decreases the likelihood of contamination by isolated or thin clouds. Third, buoy samples are discarded if the change in their insolation values with respect to the previous or subsequent value is greater than the expected change in the top of the atmosphere shortwave over that same time interval, plus some uncertainty. This uncertainty was set at 15 (30) Wm^{-2} for $\cos(\theta_o)$ greater (less) than 0.22[1]. The last criterion filters out any values that are undergoing rapid changes which are likely to be associated with the motion of scattered clouds. Once the data have been filtered using the above criteria, the remaining $SW_a\downarrow$ values are normalized to the same mean sun-earth distance through a division by $(d_m/d)^2 = \varepsilon$, where d_m (d) is the mean (instantaneous) earth-sun distance. These values are then fit against $\cos(\theta_o)$ using a least-squares polynomial regression (Appendix A). This method will be referred to as the direct-fit method.

The second method for calculating the clear-sky flux has been developed by Collins et al. (1995). This scheme was formulated independently of the buoy data and combines both modeling and empirical components in order to derive a relation between clear-sky atmospheric transmission and $\cos(\theta_o)$ (Appendix A). The clear-sky atmospheric transmission is the ratio of the downwelling clear-sky flux at the surface to the flux at the top of the atmosphere. The downwelling clear-sky flux is calculated using the procedure for net clear-sky flux from Li et al. (1993) along with the method for calculating the clear-sky surface albedo from Li and Garand (1994). This method will be referred to as the CET method.

The determination of α_c is taken from the ocean-surface albedo model of Briegleb et al. (1986). The model is an empirical fit of α_c versus θ_o and is based on the measurements of clear-sky ocean albedo by Payne (1972). The determination of α_a is based on a linear weighting of α_c and the value for the ocean surface albedo associated with diffuse irradiance (e.g., heavily overcast skies), specified here as α_d equal 0.06. Payne's measurements show that this latter value is fairly invariant (0.061±0.005) with respect to solar zenith angle,

[1]These threshold values were chosen somewhat arbitrarily but were the lowest values that still allowed the full range of $\cos(\theta_o)$ to be resolved by the remaining points.

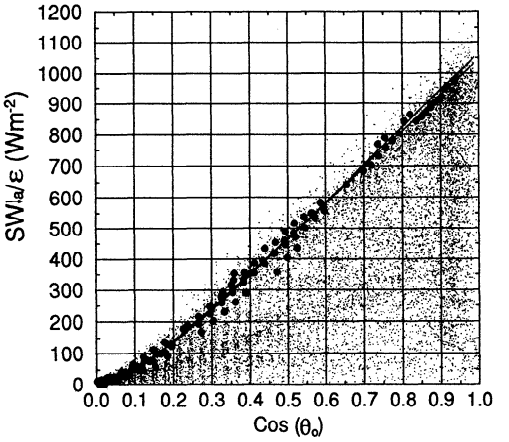

Figure 1. Downwelling surface shortwave measurements from the IMET buoy, normalized to the mean earth-sun distance, plotted against the cosine of the solar zenith angle. Each point represents a 7.5 minute average flux. Circles are the shortwave measurements that pass the cloud screening procedures described in the Methods section. The lower (upper) line shows the clear-sky flux derived from the direct-fit (CET) method (see Methods section and Appendix A).

wind speed, etc. The exact expression used is analogous to that developed by Collins et al. (1995) and is given by:

$$\alpha_a = \alpha_c + [1 - \min(SW_a\downarrow, SW_c\downarrow) / SW_c\downarrow] (\alpha_d - \alpha_c) \qquad (3)$$

Results

Figure 1 shows a scatter plot of all the daytime $SW_a\downarrow$ observations from the IMET buoy, normalized by ε, versus $\cos(\theta_o)$, along with those observations remaining after the direct-fit cloud screening criteria are applied. The scatter in the cloud-screened fluxes at each value of $\cos(\theta_o)$ is believed to be due to variations in atmospheric water vapor and aerosols, or due to optically thin or isolated clouds that were not filtered out The regression for the direct-fit of $SW_c\downarrow/\varepsilon$ along with the CET estimates are also shown in Fig. 1. The high level of agreement between the two estimates provides some assurance that the cloud screening procedures seem to be effective and that the CET model assumptions appear to be sound. Given this good agreement, it is not surprising that the two time series of $SW_c\downarrow$, and thus C_{sd}, derived from the direct-fit and CET methods also show good agreement. The correlation is over 99.9%, the root-mean-square difference is 6.8 Wm^{-2}, and the mean bias is 4.6 Wm^{-2}. Averaging $SW_c\downarrow$ over the entire buoy time series gives 309.8 (314.6) Wm^{-2} for the direct-fit (CET) method. Time series statistics for C_{sd} are given in Table 1.

In order to calculate C_{su} and C_{sn}, it is necessary to first calculate α_c, and then use it along with the corresponding values of $SW_a\downarrow$ and $SW_c\downarrow$ in Eq. 3 to calculate α_a. The mean values (day plus night) of the C_{su} time series derived from the direct-fit and CET methods are both about –4 Wm^{-2}, while the mean values of the C_{sn} time series are –103 Wm^{-2} and –107 Wm^{-2}, respectively. These estimates are in good agreement with the value reported by Ackerman et al. (1994) using land-based radiometers at Kavieng. Additional statistics on the C_{su} and C_{sn} time series are given in Table 1.

Figure 2 shows the time series of C_{sn} derived from the direct-fit method. The thick line is a 24-hour box-average of the 7.5 minute data. The high resolution data exhibit extremely large

Table 1. Comparison of Direct-Fit (DF) and CET Methods

	C_{sd}		C_{su}		C_{sn}	
Method	DF	CET	DF	CET	DF	CET
Mean	-106.4	-111.2	-3.9	-4.0	-102.5	-107.2
Max.	201.4	198.2	23.5	22.4	191.4	188.3
Min.	-1009.9	-1028.3	-34.7	-35.4	-986.5	-1004.4
St.Dv.	194.4	198.8	7.8	8.0	190.2	194.6
Bias	4.8		0.1		4.7	
RMS	7.0		0.6		6.8	
Corr.	99.96		99.78		99.96	

excursions, with peak values near -1000 Wm^{-2}, and many occurrences of positive cloud forcing. These positive values range up to almost +200 Wm^{-2}, and are the result of side-wall reflection from broken clouds that exceeds the diffuse clear-sky flux from Rayleigh scattering. The 24-hour averaging removes these positive values and reduces the cloud forcing range to between -11 and -246 Wm^{-2}. Visual inspection indicates variability at many time scales, particularly at 10-15 days. The IOP days from which the "clear-sky" points shown in Fig. 1 are extracted are indicated by diamonds at the top of Fig. 2 (see discussion on uncertainties below).

While the two estimates of C_{sn} discussed above are in good agreement, each has uncertainties. One of the largest uncertainties that applies to both methods stems from changes in the atmospheric path length associated with variability in water vapor. To determine the magnitude of this uncertainty, we have used the Li et al. (1993) algorithm to compute the variance of $SW_c\downarrow$ associated with the observed variability in atmospheric water vapor. The variability in water vapor was determined from the SSM/I observations. This data set has 270 observations overlapping the IOP with a mean value of 5.0 cm and a standard deviation of 0.58 cm. These values compare well with those obtained from the radiosondes at Kavieng for the same period (mean=5.3 cm; σ=0.58 cm; N=453). For $\cos(\theta_o)$ between 0 and 1, in increments of 0.05, the downwelling insolation has been computed over the full range of the SSM/I water vapor values (3.0-6.6 cm). The resulting output values of $SW_c\downarrow$ are weighted by the probability of occurrence of the input water vapor value used. The mean and standard deviation of these weighted $SW_c\downarrow$ values are calculated for each $\cos(\theta_o)$ bin[2]. The standard deviations are then added and subtracted from the C_{sd} estimations to determine the uncertainty in C_{sn} produced by the variability of water vapor. Independent of the method, the resulting uncertainty in C_{sn} was ± 3 Wm^{-2}. Uncertainties due to variability in aerosols (as well as other atmospheric constituents) would also influence the estimates of C_{sn}. However, determining the magnitude of this influence is difficult to assess with any degree of certainty due to the lack of aerosol observations. Errors associated with our estimates of α_a have a fairly small impact; e.g., if α_a is set to α_d (α_c), the estimates of C_{sn} differ by about +3 (-1) Wm^{-2}.

Other uncertainties exist in the estimates which are method specific. For the direct-fit method, these mainly stem from the cloud filtering procedure. For example, some of the clear-sky samples lying below (above) the regression may be associated with weakly reflecting clouds (broken cloud effects) which would have the effect of underestimating (over-estimating) $SW_c\downarrow$ and thus underestimating (overestimating) C_{sn}. Removing the cloud filtering requirement that the satellite scene before and after the current scene also have their cloud flags equal to zero yields 200% more clear-sky points (i.e., circles in Fig. 1), 55 more days with clear-sky observations (i.e., diamonds in Fig. 2) but a minor change in the regression and thus the mean C_{sn} value (-102 Wm^{-2}). Likewise, removing the second cloud filtering requirement regarding the satellite visible reflectance yields 50% more clear-sky points, 7 more days with clear-sky observations, but only a minor change in the mean C_{sn} value (-100 Wm^{-2}). Uncertainties specific to the CET method include the specification of the solar constant and a 10 Wm^{-2} standard error quoted by Li et al. (1993) on the parameterization underlying the CET method.

Discussion

The values of C_{sn} derived above raise two important questions. First, how do the mean C_{sn} values compare to the mean values of the other surface heat fluxes derived from the IMET buoy? Second, how do these IOP values compare with climatology? With respect to the first question, the mean values of the sensible, latent and net longwave fluxes for the IOP from the IMET buoy data are -9, -108.5 and -58 Wm^{-2}, respectively (Weller, R. and S. P. Anderson, 1995: Surface meteorology and air-sea fluxes in the western equatorial Pacific warm pool during the TOGA Coupled Ocean-Atmosphere Response Experiment, Submitted to J. Climate). Thus for the IOP, the shortwave cooling effect from clouds was comparable to the cooling effect from the latent heat flux, and considerably larger than the cooling from the other surface heat flux terms.

[2]The mean values are nearly identical to the values represented by the upper line in Fig. 1, while the standard deviations follow: $\sigma(SW_c\downarrow) = 0.08 + 12.9\cos(\theta_o) - 5.0\cos^2(\theta_o)$, to within 99.9%.

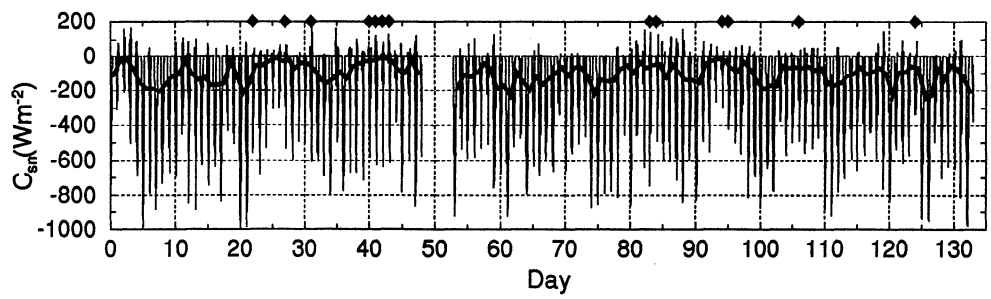

Figure 2. Time series of net shortwave cloud forcing at the surface (C_{sn}) derived from the 7.5 minute data (thin line) along with the 24-hour box-average of the 7.5 minute data (thick line). The diamonds at the top of the plot indicate the time periods from which the clear-sky samples in Fig. 1 are taken. Day 0 corresponds to October 22, 1992.

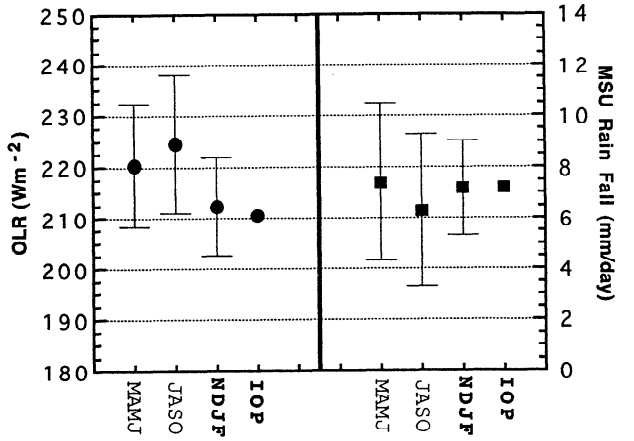

Figure 3. Climatological and average IOP values of OLR (circle; left axis) and MSU rain rate (square; right axis). The climatological values are for three seasons, Mar-Jun (MAMJ), Jul-Oct (JASO) and Nov-Feb (NDJF). The error bars represent the standard deviations associated with the "seasonal" mean values. The IOP values correspond to the mean values from November, 1992 through February, 1993.

This brings us to the second question. Recently, Ramanathan et al. (1995) made a climatological estimate of C_{sn} for the western Pacific Ocean in order to determine the ratio of the shortwave cloud forcing at the surface and the top of the atmosphere. Due to the lack of observations, Ramanathan et al. determined C_{sn} from the residual of a surface heat budget calculation, in which all other terms were estimated directly. They reported a value of -100 Wm^{-2}. In their study, this had important ramifications, since the top of the atmosphere shortwave cloud forcing measured by the Earth Radiation Budget Experiment satellite is only -66 Wm^{-2}. While most model calculations of this cloud forcing ratio are on the order of 1.1, these values give a ratio of 1.5, which indicates that significantly more shortwave absorption is occurring in the atmospheric column than is accounted for in most model calculations (Cess et al., 1995).

In the above context, it is interesting to determine how representative the COARE period is with respect to climatology, and thus how our estimates of C_{sn} might compare to the climatological value. One way to assess this is by comparing the mean values of available cloud proxies over the IMET buoy during the IOP with their climatological values. Figure 3 shows the mean OLR and MSU rain rate for the period November, 1992 to February, 1993, along with the climatological values for three four-month seasons The climatological values are determined by averaging each four month "season", and then determining the mean value of these 21 (15) "seasons" for OLR (MSU rain rate). The standard deviations of these "seasonal" values are represented by the error bars. The results in this figure indicate that the cloudiness associated with the COARE IOP was very similar to climatology. This suggests that our estimates of C_{sn} may be fairly representative of the climatological value, and it lends support to the climatological value derived indirectly by Ramanathan et al. from energy budget considerations.

Acknowledgments. This research was supported by NSF grants ATM-94-20833 (DW), ATM-94-05024 (WC), and OCE-9110559 (SA).

Appendix A

a) Direct-fit method:

$$SW_c\downarrow(\mu)=\varepsilon(1.333+345.203\mu+2043.370\mu^2-2199.560\mu^3+860.286\mu^4);\ \text{where}\ \cos(\theta_o)=\mu.$$

The bias, root-mean-square error and correlation between the above approximation and the data in Fig. 1 are 0 Wm^{-2}, 18.9 Wm^{-2} and 99.8%, respectively.

b) CET method:

$SW_c\downarrow(\mu) = S_o\,\varepsilon\,\mu\,\tau(\mu)$; where S_o is 1365 Wm^{-2} and $\tau(\mu)=0.120+3.216\mu-8.300\mu^2+12.083\mu^3-8.987\mu^4+2.652\mu^5$.

References

Ackerman, T. P, C. N. Long, A. T. George and J. A. Valero, 1994: The Surface Radiative Budget at Kavieng, PNG During the TOGA COARE Period. Summary Report of the TOGA COARE International Data Workshop. Toulouse, France. 2-11 August, 1994.

Briegleb, B. P., P. Minnis, V. Ramanathan, E. Harrison, 1986: Comparison of Regional Clear-Sky Albedos Inferred from Satellite Observations and Model Computations, *J. Clim. Appl. Met.*, 25, 214-226.

Cess, R. D., M. H. Zhang, + 18 others, 1995: Absorption of Solar Radiation by Clouds: Observations Versus Models. *Science*, 267, 496-499.

Collins, W. D., F. P. J. Valero, P. J. Flatau, D. Lubin, H. Grassl, P. Pilewskie, 1995. The Radiative Effects of Convection in the Tropical Pacific. *J. Geophys. Res.*, In Press.

Gruber, A. and A. F. Krueger, 1984: The Status of the NOAA Outgoing Longwave Radiation Data Set. *Bull. Am. Met. Soc.*, 65, 958-962.

Li, Z., H. G. Leighton, K. Masuda, and T. Takashima, 1993: Estimation of SW Flux Absorbed at the Surface from TOA Reflected Flux. *J. Climate*, 6, 317-330.

Li, Z. and L. Garand, 1994: Estimation of Surface Albedo from Space: A Parameterization for Global Application. *J. Geophys. Res.*, 99, 8335-8350.

Payne, R. E., 1972: Albedo of the Sea Surface. *J. Atmos. Sci.*, 29, 959-970.

Ramanathan, V., B. Subasilar, G. J. Zhang, W. Conant, R. D. Cess, J. T. Kiehl, H. Grassl and L. Shi, 1995. Warm Pool Heat Budget and Shortwave Cloud Forcing: A Missing Physics? *Science*, 267, 499-503.

Rossow, W. B. and R. A. Schiffer, 1991: ISCCP Cloud Data Products. *Bull. Am. Met. Soc.*, 72, 2-20.

Schluessel, P. and W. J. Emery, 1990: Atmospheric Water Vapour over Oceans from SSM/I Measurements. *Int. J. Rem. Sens.*, 11, 753-766.

Spencer, R. W., 1993: Global Oceanic Precipitation from the MSU during 1979-91 and Comparisons to Other Climatologies. *J. Climate*, 6, 1301-1326.

Webster, P. J. and R. Lukas, 1992: TOGA COARE: The Coupled Ocean-Atmosphere Response Experiment. *Bull. Am. Met. Soc.* 73, 1377-1416.

S. Anderson, Department of Physical Oceanography, Woods Hole Oceanographic Institution, Woods Hole, MA 02543

W. Collins, Center for Clouds, Chemistry and Climate, Scripps Institution of Oceanography, La Jolla, CA 92093

D. Waliser, Institute for Terrestrial and Planetary Atmospheres, State University of New York, Stony Brook, NY 11794-5000

(Received September 4, 1995; revised December 13, 1995; accepted December 29, 1995.)